Nucleic Acids Research, Vol. 19, No. 19 5313–5320

Alternative tertiary structure attenuates self-cleavage of the ribozyme in the satellite RNA of barley yellow dwarf virus

W.Allen Miller and Stanley L.Silver
Plant Pathology Department and Molecular, Cellular and Developmental Biology Program, Iowa State University, Ames, IA 50011, USA

Received June 27, 1991; Revised and Accepted August 31, 1991

ABSTRACT

A self-cleaving satellite RNA associated with barley yellow dwarf virus (sBYDV) contains a sequence predicted to form a secondary structure similar to catalytic RNA molecules (ribozymes) of the 'hammerhead' class (Miller *et al.*, 1991, *Virology* 183, 711–720). However, this RNA differs from other naturally occurring hammerheads both in its very slow cleavage rate, and in some aspects of its structure. One striking structural difference is that an additional helix is predicted that may be part of an unusual pseudoknot containing three stacked helices. Nucleotide substitutions that prevent formation of the additional helix and favor the hammerhead increased the self-cleavage rate up to 400-fold. Compensatory substitutions, predicted to restore the additional helix, reduced the self-cleavage rate by an extent proportional to the calculated stability of the helix. Partial digestion of the RNA with structure-sensitive nucleases supported the existence of the proposed alternative structure in the wildtype sequence, and formation of the hammerhead in the rapidly-cleaving mutants. This tertiary interaction may serve as a molecular switch that controls the rate of self-cleavage and possibly other functions of the satellite RNA.

INTRODUCTION

Some viruses in the nepo-, luteo- and sobemovirus groups contain small satellite RNAs that replicate via a rolling circle mechanism (reviewed in 1,2). Circular and multimeric forms of these RNAs undergo self-cleavage at a specific site to generate the monomeric form that predominates in the virus particle. This self-cleavage is catalyzed by a subset of the satellite RNA sequence (ribozyme) flanking the cleavage site that is predicted to fold into a hammerhead-shaped structure (3,4; reviewed in 5). One viroid, avocado sunblotch viroid (ASBV, 6), and the transcripts of satellite 2 DNA of newt also self-cleave at a hammerhead structure (7). The consensus hammerhead structure consists of three short helices, whose sequences are not conserved, joined together by short single-stranded regions, most of which are conserved at the primary structure (sequence) level. In contrast, the loops connecting the distal portions of the helices can be varied in sequence (8), or removed altogether (9,10), without loss of ribozyme activity. Much effort has been devoted to elucidation of the structure-function relationships of hammerhead ribozymes, including mutagenesis of the helices and the conserved single-stranded bases (11–16).

A self-cleaving satellite RNA was recently reported associated with the RPV serotype of barley yellow dwarf virus (sBYDV, [17] GenBank Accession number M63666). This is the first known satellite of a member of the luteovirus group. Encapsidated sBYDV RNA is a predominantly linear monomer, 322 nucleotides (nt) long, and it encodes no long open reading frames. In being a linear molecule it more closely resembles the satellite RNA of tobacco ringspot virus (sTobRV, 2) than the satellites of the sobemoviruses (also known as virusoids) in which the circular monomer is the most abundant form.

The (−) strands of some but not all of the self-cleaving satellite RNAs also self-cleave, indicating variations in the rolling circle mechanisms (1, 2). Both the encapsidated (+) strand and the (−) strand of sBYDV RNA self-cleave (17). The (−) strand self-cleaves extremely rapidly and contains a perfect consensus hammerhead sequence flanking the self-cleavage site (5,14). The sequence flanking the cleavage site in the encapsidated (+) strand of sBYDV fits most of the consensus rules for formation of a hammerhead structure. However, the (+) polarity sBYDV hammerhead differs from other naturally occuring hammerheads in at least three features (Fig. 1). First, the trinucleotide at the 5′ side of the cleavage site is AUA, instead of GUC, which is found in all naturally occuring hammerheads except that of lucerne transient streak virus satellite (sLTSV) that cleaves at GUA (4). However, functional hammerheads have been constructed with many variations from GUC (7, 14). Second, an unpaired cytosine (C-24) is present immediately 3′ to the conserved single-stranded CUGANGA sequence, and an unpaired adenine (A-73) occurs immediately 5′ of the conserved GAAAN sequence. In almost all other cases, bases in these positions are hydrogen bonded to form the first pair of the vertical helix 2 (5,14). No others have an unpaired base analogous to A-73.

The third and most striking, unusual feature is the subject of this paper: the 'loop' (L1) connecting strands of helix 1 (H1) would be expected to pair with a sequence (L2a), which is drawn as a single-stranded loop in the hammerhead conformation in compound helix 2 (Fig. 1). The calculated stability of the helix formed by L1-L2a base pairing ($\Delta G = -10.1$ kcal/mol) is the strongest in the entire satellite RNA. Thus, structures containing the L1-L2a helix may be energetically preferred, and loops L1 and L2a would not be expected to remain single-stranded as

shown in the hammerhead conformation in Fig. 1A. Because the formation of the L1-L2a helix does not replace any of the base pairing involved in hammerhead formation, it may be possible for all helices to remain intact, giving the unusual pseudoknot-like structure shown in Fig. 1B. This structure contains an interesting set of three coaxially stacked helices, the central one being the L1-L2a helix. Although such a structure may not be possible due to torsional constraints, we sought to determine if it could form by observing the effects of mutagenesis of the putative L1-L2a helix on the self-cleavage rate, and on overall secondary and tertiary structure.

MATERIALS AND METHODS

Synthesis of wildtype and mutant self-cleavage structures

RNA molecules were synthesized by *in vitro* transcription of sequences in phagemid pGEM3Zf(−) (Promega, Madison, WI). Mutations were introduced by the method of Kunkel (18), using a kit from Biorad (Richmond, CA). Plasmid pSS1 contained the wildtype (+) strand sBYDV hammerhead sequence: bases 310−322 and 1−89 of the satellite sequence (Figs 1 and 2). Cleavage occurs between bases 322 and 1. pSS1 was derived from the slightly larger plasmid pPCS1 (17) by site-directed mutagenesis with the primer: 5'GTTATCCACGAAATAGG-A'TC*CTATAGTGAGTCGTATTAC* 3'. Bases 5' of the apostrophe are complementary to satellite RNA sequence. The complement of the T7 RNA polymerase promoter is shown in italics. This resulted in deletion of 25 vector-derived bases and 11 satellite RNA bases not involved in formation of the hammerhead structure. Transcripts of *Xba*I-linearized pSS1 and mutants contained vector bases GGA and CUCUAG at the 5' and 3' ends, respectively. The following plasmids containing mutant sBYDV self-cleavage structures were constructed with the indicated primers. (See maps and sequence alterations in Fig. 2). pM1: 5' CGTCGTCAGACAGTAGGGCCTCTGTTATCCACGAA-3'; pM2: 5' CCAGCCTTCTAGTCCGGCCCGATACGTCGT-CAGAC 3'; pM19: 5' AGACAGTACGAGCTCTGTTATC 3'; pM20: 5' TTCTAGTCCGCTCGGATACGTCG 3'; pM5: 5' GGATTTCTGTATCTATT'GATACGTCGTCAGAC 3'. Underlining indicates base changes, and the apostrophe indicates site of deletion. All plasmids were sequenced in the transcribed regions by the dideoxy method with Taq polymerase (Promega). In our nomenclature, a plasmid and its *r*anscript are named similarly except that the 'p' of the plasmid name is omitted in designating the transcript.

Self-cleavage assays

[α-^{32}P]UTP-labeled RNAs were transcribed *in vitro* as described previously (17) from *Xba*I-linearized plasmids. Uncleaved transcripts were purified by elution (19) after electrophoresis of transcription products on an 8% polyacrylamide, 7M urea gel. Self-cleavage reactions contained approx. 10,000 cpm gel-purified, uncleaved transcription product, 1 μg/μl tRNA, 50 mM Tris, pH 7.5, and 10 mM $MgCl_2$. Reactions were started by addition of the $MgCl_2$. To stop the reaction, 5 μl aliquots were removed at designated time points, added to an equal volume of 7 M urea, 30 mM EDTA and immediately frozen at −80°C. Samples were thawed and denatured by boiling for one min immediately prior to electrophoresis on 8% polyacrylamide, 7 M urea sequencing-type gels. Bands were cut out and radioactivity determined by liquid scintillation counting.

Synthesis of end-labeled RNA

Each of the steps below was terminated by making solutions 50 mM in EDTA, extracting once with phenol:$CHCl_3$ (1:1), and ethanol precipitation in 2M ammonium acetate pH 6.2. *Step 1:* Unlabeled transcripts were synthesized as described above except that the reactions contained: 5−15 μg of linearized template, 0.5 mM of all four NTPs, 100 units RNasin, in a 100 μl final reaction volume. *Step 2:* Transcription products were treated with 5 units calf intestinal phosphatase for 10 min in the absence of magnesium as in (20). *Step 3:* End-labeling reactions (50 μl) contained dephosphorylated transcript, 40 units RNasin, 100 μCi [γ-^{32}P]ATP (3000 Ci/mmole), 10 units polynucleotide kinase, 50 mM Tris, pH 8.0, 10 mM $MgCl_2$. To minimize self-cleavage during labeling, $MgCl_2$ was added last and reactions were incubated only 5 to 10 min before addition of EDTA to stop the reaction. *Step 4:* Uncleaved transcripts were purified by gel electrophoresis as already described.

Nuclease digestion

All nucleases except V1 (Pharmacia, Milwaukee, WI) were from BRL (Gaithersberg, MD). Nuclease digestions were under the same conditions of temperature and solution used in the self-cleavage assays. Reactions (5 μl) contained approx. 10,000 cpm per reaction of gel-purified, end-labeled uncleaved RNA, 1 μg/μl tRNA, 50 mM Tris, pH 8.0, 10 mM $MgCl_2$, and either 0.2 units V1 nuclease, 0.1 units T2 nuclease, 0.2 units T1 nuclease, or water. Nuclease treatment was initiated 20 to 50 s after addition of $MgCl_2$. After 5 min at 37°C, reactions were terminated by adding an equal volume of 7M urea, 30 mM EDTA and freezing at −80°C. Products were separated on 12% polyacrylamide gels containing 7M urea. Sequencing reactions (T1 and ϕM nucleases) under denaturing conditions (21,22) and ladder formation by partial alkaline hydrolysis were performed by using a kit from BRL.

RESULTS

Self-cleavage of wildtype and mutant RNAs

Transcripts from a plasmid (pPCS1) spanning the (+) strand cleavage site were shown previously to self-cleave (17). However, the rate of cleavage and the effects of a large number of extraneous bases were unknown. To allow transcription of an RNA that contained the hammerhead sequence with minimal vector-derived bases, 36 bases were deleted from pPCS1 to create pSS1 (Fig 2). The RNA transcript (SS1) from *Xba*I-linearized pSS1 contained only 3 vector-derived bases at the 5' end and at most 6 at the 3' end (Figs. 2A, 5). Optimal conditions for self-cleavage of SS1 were 50 mM Tris-HCl, pH 7.5, 10 mM $MgCl_2$, at 37°C. The reaction showed a broad magnesium optimum, and little sensitivity to temperature or denaturation treatments such as boiling and snap cooling (4) prior to addition of Mg^{2+} (data not shown). The cleavage products of all the transcripts were as expected: a 120 nt full-length fragment, a 101 nt 3' fragment, and a 19 nt 5' fragment (Fig. 3). The intensity of the full-length band decreased as the intensities of the fragments increased with time.

Transcript SS1 cleaved with an approximate half-life of 1500 to 2500 min as calculated by extrapolation of several separate experiments (Figs. 2, 3). To determine if the slow rate of cleavage was due to formation of the alternative base pairing (L1-L2a; Fig. 1), the potential to form this helix was disrupted by

mutagenesis. Two three-membered sets of mutants were constructed (Fig. 2). Each set included transcripts with alterations to L1, L2a, or to L1 and L2a on the same molecule such that potential base pairing, but not wildtype sequence was restored in the double mutant. In an additional mutant (M5), bases 30–63, including the L2a region, were deleted (Fig. 2). This prevented formation of the L1-L2a helix, and resulted in a hammerhead similar in size to those of the sobemovirus satellites (virusoids), sTobRV (5), and sBYDV RNA (−) strand (17).

Mutant set **I** (mutants M1, M2, and M1/2), was designed to conserve the 100% G+C content of L1 and L2a. Three bases were changed in either L1 or L2a, or both L1 and L2a. The half-lives of mutant RNAs M1 and M2, in which the proposed L1-L2a base pairing was disrupted, were 310 and 48 min, respectively (Figs. 2, 3). The double mutant M1/2 did not self-cleave detectably. In contrast to mutant set **I**, set **II** was chosen after exhaustive computer searches (23) of many sequences containing different mutations predicted that this set of mutations should form no significant unintended base pairing. Mutant set **II** (M19, M20 and M19/20) was constructed by introducing only a single base change in either L1 or L2a, or both L1 and L2a. Each of the single mutants, M19 and M20, cleaved hundreds-fold more efficiently than wildtype (Figs. 2, 3). Seventeen percent of M19 RNA remained uncleaved after 10 hr, presumably because this proportion of the molecules folded into an inactive conformation. The double mutant M19/20 cleaved 24- to 36-fold more slowly than either of the single mutants, but at least 10-fold faster than wildtype. Mutant M5 also cleaved quite rapidly (Figs. 2, 3). The full-length transcript (86 nt) and the 3′ (67 nt) and 5′ (19 nt) fragments migrated as expected.

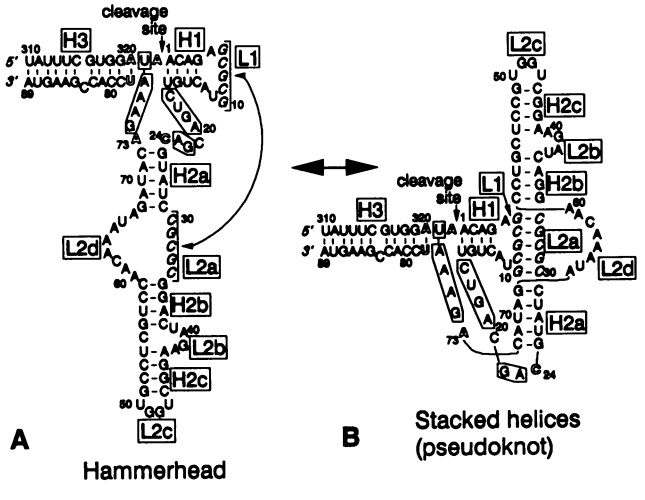

Figure 1. Proposed alternative structures for the self-cleaving ribozyme in sBYDV (+) strand RNA. Boxed bases are conserved among all hammerheads (5). Bases that differ from consensus are shown in outlined text. Numbering of nucleotides is based on the full-length satellite RNA (17). Numbering of the three major helices (H1, H2, H3) of the hammerhead is as in (4,5). Single-stranded regions (loops) are prefixed with L. The individual helices and loops within compound stem-loop 2 are labeled as lettered subsets. Bases in loops L1 and L2a expected to form the additional helix are in italics. Cleavage structure is drawn as a hammerhead (**A**) without L1-L2a base pairing, and in the alternative conformation (**B**), in which L1 and L2a base pair without disruption of other helices to form a pseudoknot with three stacked helices. Because of difficulties in two dimensional representation, lines indicating phosphodiester bonds have been added as necessary. Note the coaxial alignment of three helices in **B** with the helix derived from L1 and L2a in the center.

Nuclease Sensitivity

The next set of experiments employed structure-sensitive nucleases to determine whether the overall tertiary structure exists as predicted in Fig. 1B. 5′ end-labeled transcripts were partially digested with nucleases T2 (cuts all single-stranded bases [24]), T1 (cuts single-stranded guanosine nucleotides), or V1 (cuts double-stranded and some base-stacked regions [25,26]), under conditions identical to those used in the cleavage assays. To avoid misleading secondary cleavages, enzyme concentrations were adjusted so that the RNA was cleaved less than once per molecule, on average. The digestion times were short enough (5 min) to allow analysis of the RNA structure before it self-cleaved. The possibility that the nuclease digestion reveals structures of the cleavage products is eliminated in all bands greater than 19 nt long, because self-cleavage of the 5′ end-labeled RNA would remove label from the 3′ product. Products of nucleolytic digestions of the wildtype and all the mutant transcripts were separated on denaturing gels alongside cleavage products obtained with nucleases T1 and ϕM (cuts after A and U residues) under fully denaturing conditions (Fig. 4). A wide variation in nuclease susceptibility of phosphodiester bonds under self-cleavage conditions relative to denaturing conditions indicated regions of strong structure. Nuclease T2 cut single-stranded G residues only weakly, compared to its activity on the other three bases. The prominant 19 base band in all samples (including those lacking nuclease) except M1/2, that were digested in self-cleavage conditions is the 5′ self-cleavage fragment. It migrated exactly

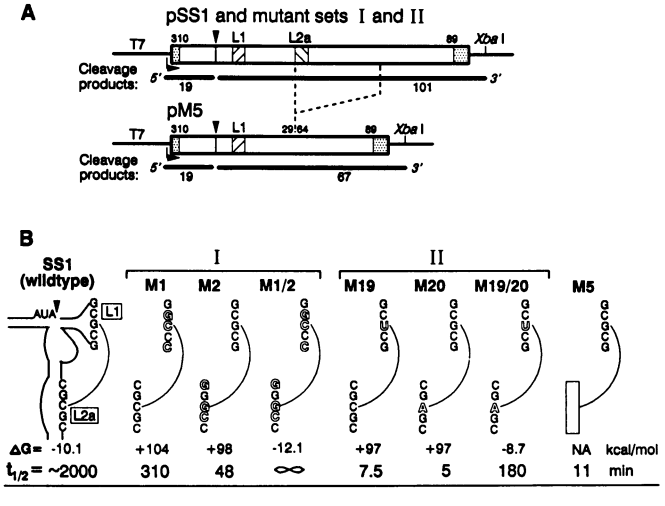

Figure 2. A. Maps of inserts in transcription plasmids. Large bold box represents sBYDV RNA sequence; shaded regions (flanking bases 310 and 89) are not required for hammerhead formation. Horizontal arrow marks the transcription start site; vertical arrowhead indicates self-cleavage site. Expected cleavage products of transcripts generated by T7 polymerase-catalyzed transcription of *Xba*I-linearized DNA are shown as bold lines below map. Sizes of transcripts (in nt) are indicated below each one. Specific changes in L1 and L2a (shaded with diagonal lines) in mutant sets **I** and **II** are shown in panel B. Dashed lines indicate region (bases 30–63) of pSS1 that was deleted in pM5. **B.** Schematic representations of mutants with base changes (outlined text) in the putative L1-L2a helix. Mutants are grouped into sets **I** and **II** as described in the text. Only the sequences of L1 and L2a are shown. Their positions in the hammerhead are shown in SS1 (wildtype) at left. Empty box in mutant M5 represents deletion of L2a sequence. The name of each mutant (above) and free energies (below) of potential L1-L2a helices are indicated. Helices were identified and free energies calculated by using the RNA Structure Editor (RNASE) computer program (23) which used the parameters in (40). NA = not applicable. The bottom line shows the half-lives ($t_{1/2}$) of uncleaved RNAs calculated from graphs in Fig. 3.

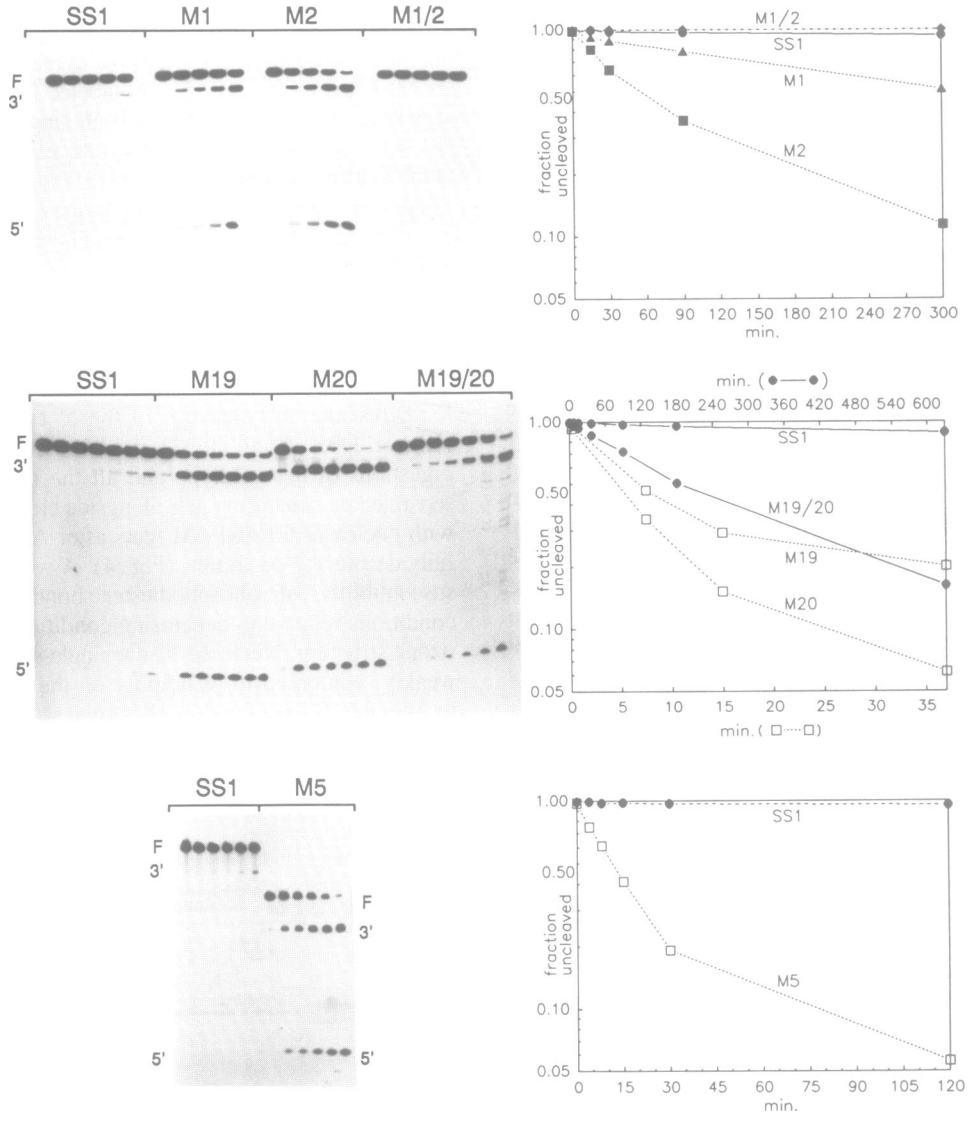

Figure 3. Self-cleavage of wildtype and mutant RNAs. *Left:* Autoradiographs of transcripts after incubation in self-cleavage conditions for times shown in graphs at right, and denaturing polyacrylamide gel electrophoresis. Mobilities of full-length (F) transcript, and 3′ and 5′ fragments are indicated. *Right:* Semilog plots of fraction of full-length transcript that remains uncleaved were calculated from radioactivity in bands of autoradiographs at left. In the middle graph, note that M19 and M20 are plotted against a different scale (bottom) than are SS1 and M19/20 (top scale). SS1 was included as a standard in all assays.

as expected on the basis of the T1 and ϕM sequencing ladders. Some minor nonspecific degradation is visible in the untreated lanes (*e.g.*, M19, M5) that cause misleading bands that are not a result of nuclease digestion in the nuclease-treated lanes.

The sites and frequency of nuclease cutting in all the RNA molecules are shown in Fig. 5. In all transcripts, predicted helix 3 was cleaved strongly by nuclease V1 and not by nucleases T1 or T2. Phosphodiester bonds in putative helix 1 were susceptible to both single- and double-strand-specific nucleases in all instances. In contrast, loop L1 was much more susceptible to single-strand-specific nucleases in most of the single mutants in which L1-L2a base pairing was expected to be disrupted (M2, M19, M20, M5), than in those in which L1-L2a base pairing was predicted (SS1, M1/2, M19/20). This is especially noticeable when the T1 digests under cleavage and denaturing conditions are compared across all the RNAs (Fig. 4). Concomitantly, in the double mutants, nucleotides in L2a were digested somewhat more readily by nuclease V1 than were the L2a bases in the single mutants. In all RNAs, loops L2b, L2c, and L2d were highly susceptible to single-strand-specific nucleases. Predicted helix H2a was generally more susceptible to V1, with the exception of M1 in which it appeared highly single-stranded. H2b and H2c were not cleaved well by any nucleases, except for H2b in M2 and M1/2 which were cleaved unexpectedly by single strand-specific nucleases. The conserved CUGANGA loop was sensitive to single-stranded nucleases in all but M1. Thus, the nuclease cleavage pattern of M1 RNA was radically different from that expected, unlike the patterns generated by the other transcripts.

DISCUSSION

Effects of mutations on self-cleavage rate

By showing that disruption of the potential L1-L2a helix dramatically increased self-cleavage activity and that restoration of the potential helix with a new sequence reduced activity, we have provided strong evidence for the existence of the helix in

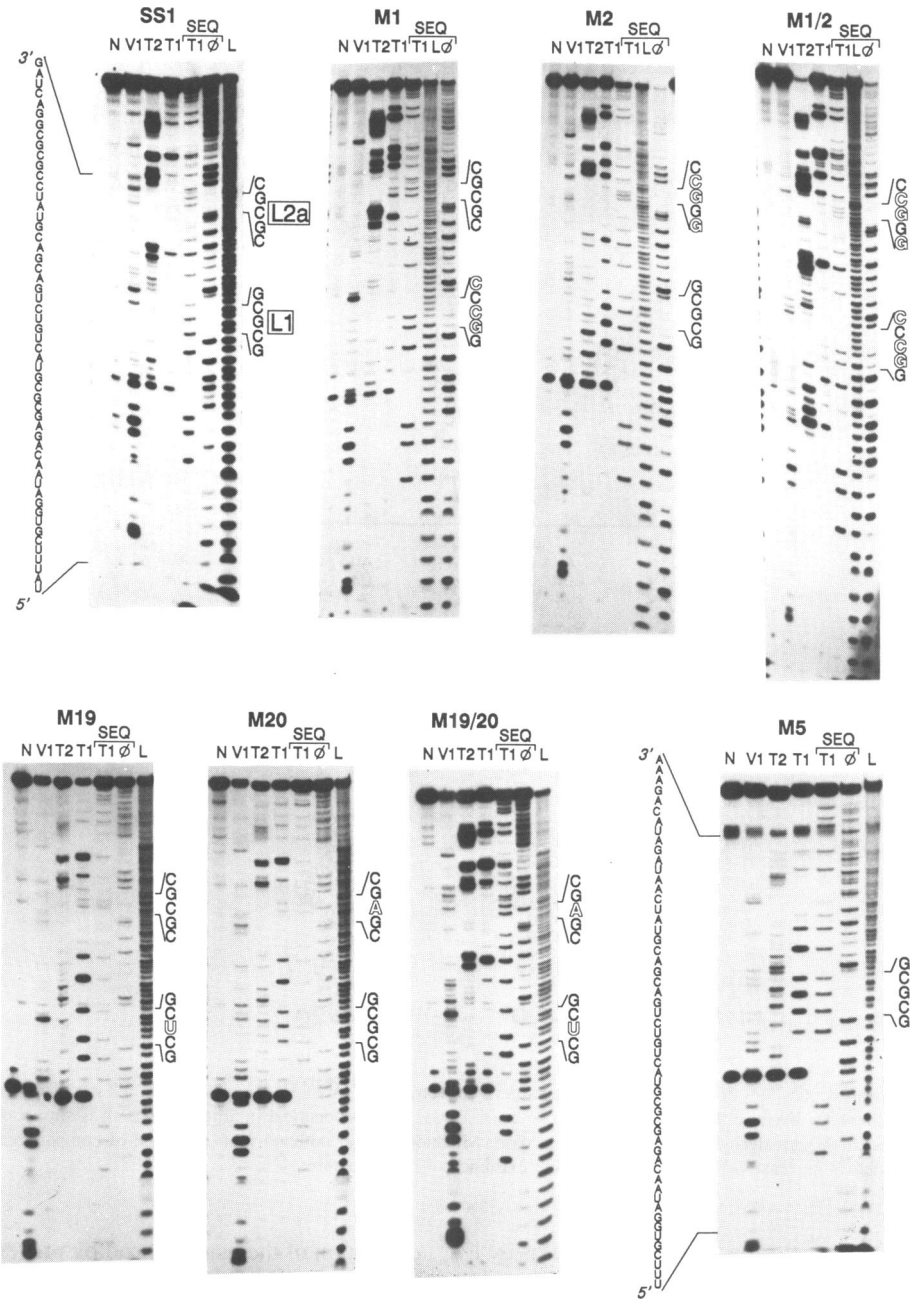

Figure 4. Autoradiographs after incubation of wildtype and mutant RNAs with the indicated nucleases. Products were analyzed on 12% polyacrylamide, 7M urea gels. Lanes are labeled for the enzyme treatment, except that lanes marked **N** had no enzyme added and **L** indicates partial alkaline hydrolysis ladder. ϕ indicates ϕM digest which cut A residues slightly more strongly than U's. **SEQ** indicates nuclease digestions under denaturing (sequencing) conditions. Other digests were in self-cleavage conditions. Products of the V1 digest ran one base more slowly than those in the other lanes due to the absence of a 3′ phosphate (25,41). Readable sequences of SS1 and M5 are indicated alongside the autoradiographs. Positions of bases in L1 (lower set) and L2a (upper set) are indicated along side each autoradiograph. These helices are labeled beside the SS1 autoradiograph only. Bands in lanes N and V1 of M19 are shifted to the left slightly at the intense 19 nt cleavage product due to tearing of the gel.

the self-cleavage structure of sBYDV (+) strand RNA. Because disruption of this base pairing is predicted to favor formation of a hammerhead RNA, the results also support the proposal (3,4) that the hammerhead is indeed the self-cleavage structure. That different disruptions to the L1-L2a helix have different cleavage rates implies that other unpredicted folding may be taking place.

It is noteworthy that the rates of cleavage of SS1 and mutants M1/2 and M19/20 are inversely proportional to the calculated stability of helix L1-L2a (Fig. 2). Thus, we propose that an equilibrium exists between the self-cleaving hammerhead and the noncleaving stacked helix structure. Even if the latter is favored, any brief formation of the hammerhead would allow irreversible cleavage. This explains the slow but steady rates of cleavage of SS1 and M19/20. In M1/2, apparently the helix is so strong that the hammerhead never forms. The situation is somewhat analogous to the self-cleavage structure of hepatitis δ virus (HDV) RNA. Although HDV RNA shows no evident relationship to a hammerhead, it seems to form a structure in which one helix

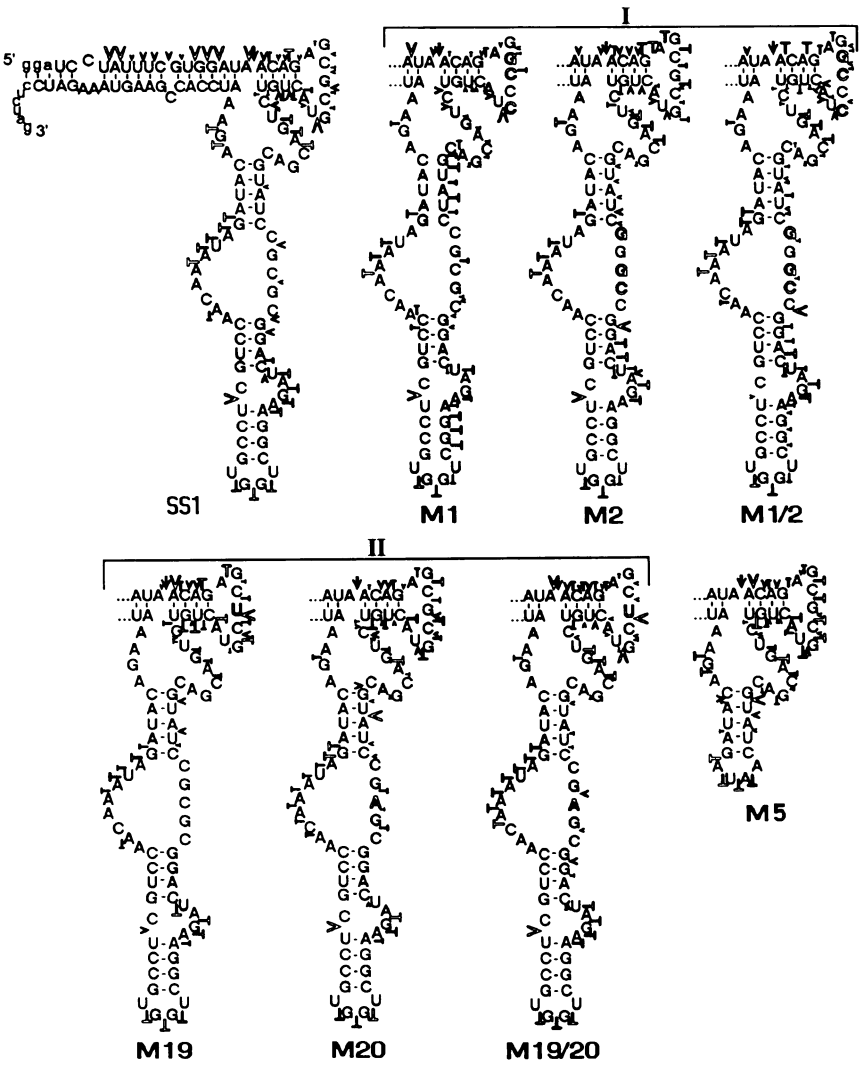

Figure 5. Locations and relative susceptibilities of nuclease cleavage sites derived from Fig. 4. **V** = V1 site, **T** = T1 or T2 site. The size of the V or T is proportional to the intensity of the band at that site. Because the digestion pattern of helix 3 was virtually identical in all constructs, it is shown only for wildtype (SS1) RNA. Mutant sets **I** and **II** are indicated. Vector-derived bases are in lower case. Mutations are in outlined font. For ease of comparison, the sequences are drawn as hammerheads regardless of whether nuclease sensitivity supported the existence of this structure.

inhibits self-cleavage (27). Denaturing conditions such as <1 mM Mg^{2+}, high temperature, or presence of urea or formamide accelerate the cleavage rate (28). However, unlike HDV RNA, the rate of sBYDV RNA cleavage does not increase at elevated temperatures such as 50°, nor does it increase at low magnesium concentrations, or after boiling and snap-cooling. Perhaps this is because the L1-L2a helix is the most stable in the molecule, and helices required for hammerhead formation (e.g. H1) would denature before L1-L2a. Of the known hammerheads (5), only the (+) and (−) strands of sLTSV have potential base pairing between the distal loops of helices 1 and 2 like (+) sBYDV. However in that case, such base pairing is not predicted to be as stable as that involved in hammerhead formation.

Nuclease Sensitivity

The self-cleavage assays of wildtype and mutant sequences do not distinguish between the following two possibilities: *(i)* the three stacked helices form as proposed in the wildtype ribozyme with no disruption of the hammerhead (H1, H2, H3) helices (Fig. 1b), and *(ii)* the L1-L2a base pairing causes major disruption of the hammerhead by preventing one or more of the hammerhead helices from forming and perhaps allowing many new helices to form. To distinguish between these possibilities, the RNAs were probed with structure-sensitive nucleases.

Nuclease sensitivity of the wildtype self-cleavage structure (SS1, Fig. 5) is, for the most part, consistent with the proposed structure. However, other than H3, predicted helices are not clearly shown by V1 digestion. This may be due to the wide variation in ability of nuclease V1 to act on certain helical regions (25,26,29). Certain regions (*e.g.*, putative helices H2b, H2c) were not cleaved by V1 nuclease, presumably due to steric hindrance in which the enzyme could not interact with nucleotides in the interior of the RNA molecule (30). In addition, some regions predicted to be single stranded were partially cut by V1, perhaps due to the ability of V1 to cut at nonpaired but stacked bases (26, 29). Helix H1 was cleaved by single- and double-strand-specific nucleases, perhaps because it 'breathes' during the nuclease treatment owing to its low stability ($\Delta G = -5.3$ kcal/mol). Thus the structural information derived from the V1 digests is somewhat limited.

Single-strand-specific nuclease digestions gave more clear-cut results than the V1 digestions. The observation that loops L2b, L2c, L2d, and the conserved CUGANGA loop (with one exception) remained sensitive to nucleases T1 and T2 provides strong evidence that the entire vertical stem-loop 2 region forms as in the proposed structures (Fig. 1). Unexpected alterations to structures of RNAs in mutant set **I** were observed (Fig. 5). The most unexpected changes were in M1 which explains why it cleaves so much more poorly than the other mutants that disrupt L1-L2a base pairing. Indeed, a computer search (23) revealed that many new helices may form as a result of the three base changes in both M1 and M2 (not shown), perhaps explaining why neither mutant cleaved as well as M19 or M20. Although the nuclease sensitivity results do not support the structure of M1 as drawn, the functional assay shows that disruption of L1-L2a still allowed the RNA to form a functional cleavage structure at least a portion of the time, causing it to cleave more readily than wildtype. Unlike M1, the nuclease sensitivity of M2 supports the existence of a functional hammerhead. Note the striking increase in sensitivity to single-stranded nucleases of loop L1 in M2 versus SS1. The disrupted helix H2b in M2 is not predicted to be essential for a functional hammerhead. Thus, it is not surprising that this RNA cleaves much more rapidly than M1.

The base changes in mutant set **II** resulted in no significant changes in nuclease sensitivity outside the predicted regions, with the exception of slight unexpected cuts in L1 by V1 in M19 and M20. Finally, M5, in which most of the entire vertical stem including L2a was deleted, behaved as predicted. This is the first use of structure-sensitive nucleases to show that hammerhead ribozymes indeed fold as predicted by the model of Forster and Symons (4).

Comparison with other hammerheads

Even the fastest-cleaving mutants do not cleave as rapidly as conventional hammerhead ribozymes such as sBYDV (−) strand (17) or sTobRV (+) strand (8). This may be due to the other deviations from consensus (Fig. 1). The AUA instead of a GUC at the 5′ side of the cleavage site is not likely to significantly reduce the rate of cleavage relative to other hammerheads. Ruffner et al. (14) showed that replacement of the G or the C of the GUC with A's at either position had only minimal effect on cleavage by an ASBV-derived ribozyme. However, when the bases of the proximal base pair of helix 2 were changed to C and A, analogous to C-24 and A-73 in sBYDV RNA, cleavage by the ASBV-derived ribozyme was reduced over one hundred-fold. Given this and similar observations with sLTSV mutagenesis (15), it is perhaps surprising that mutants M19, M20, and M5—all of which contain unpaired bases C-24 and A-73—cleave as well as they do.

The results do not prove the existence of the three stacked helices, but they support this model (Fig. 1B). This structure fits the definition of a pseudoknot (31); however, it has three instead of the usual two coaxially stacked helices. It is possible that helix H1 would be pulled apart due to torsional constraints when the L1-L2a helix forms, but the nuclease sensitivity does not correlate with this. It is possible that yet another conformation exists within the context of the full-length satellite RNA. Other examples of alternative conformations for hammerhead domains have been reported. The self-cleavage sequences in the (+) and (−) strands of sLTSV may exist in equilibrium between the hammerhead and as part of the rod-shaped full-length molecule (4). The self-cleavage sites in newt satellite 2 transcripts (32) and ASBV RNA (33) may fold differently in the context of a dimer of the full satellite RNA, compared to the sequence context of the isolated hammerhead. These RNAs have an extremely short (2 or 3 base pair) helix 3. In the minimal hammerhead context, cleavage can occur by a bimolecular double-hammerhead structure (34), whereas dimeric satellite RNA self-cleaves mostly via single-hammerheads (32,33). Thus, it will be interesting to determine the cleavage rate of dimeric sBYDV RNA. However, the sBYDV situation is quite different from the newt and ASBV in that we observed *intra*-hammerhead conformational changes rather than *inter*-hammerhead base pairing. Due to the length of helix 3, we have no reason to invoke a bimolecular double-hammerhead mechanism (35). The sLTSV alternative conformation is also unlike sBYDV in that it involves base pairing to regions outside the hammerhead domain (4). Finally, alternative conformations have also been observed when the ribozyme and substrate are located on separate molecules (13,16). Because the L1-L2a helix is the strongest uninterrupted helix in the entire satellite, and the strands are in such close proximity, we predict that the helix exists even in the context of full-length and multimeric RNAs.

The biological role of the stacked-helix structure is unknown. An intriguing possibility is that the L1-L2a helix may form left-handed Z-RNA (reviewed in 36). It contains the alternating G-C sequence required for Z-RNA. Also, torque may be imposed by the strands of the distal end of putative helix H1 on helix L1-L2a because these strands would be expected to join L1 at opposite sides of the one-half turn, 5-base L1-L2a helix. This may confer negative supercoiling that is known to favor Z-DNA (37). Z-RNA has been shown to exist in living cells (38,39), but its identity and biological role are unknown. Regardless of whether Z-RNA forms, it is possible that the stacked helix structure performs a function different from self-cleavage. Nearly half (153 nt) of the 322 nt sBYDV RNA is involved in formation of either the (+) strand or complement of the (−) strand cleavage structure. This leaves only 169 nucleotides divided into two tracts of 104 and 65 bases (17) to perform all the other functions of the satellite RNA, including an origin of replication, an origin of assembly and probably other functions. Thus, it could be envisioned that sequences within the self-cleavage structure contribute to one of these other functions, compromising the ability to self-cleave in the process. The stacked-helix may serve as a molecular switch to modulate the transition between these two functions.

ACKNOWLEDGMENTS

The authors thank Amy Morrow and Jean-Francois Bonnet for technical assistance. This work was funded by grants from the Quaker Oats Company and the Midwest Plant Biotechnology Consortium. This is Journal Paper No. J-14555 of the Iowa Agriculture and Home Economics Experiment Station, Ames; Project No. 2945.

REFERENCES

1. Symons, R.H. (1991) *Molec. Plant-Microbe Interact.* **4,** 111−120.
2. Bruening, G., Passmore, B.K., van Tol, H., Buzayan, J.M., and Feldstein, P.A. (1991) *Molec. Plant-Microbe Interact.* **4,** 219−225.
3. Forster, A.C. and Symons, R.H. (1987) *Cell* **50,** 9−16.
4. Forster, A.C. and Symons, R.H. (1987) *Cell* **49,** 211−220.
5. Bruening, G. (1989) *Methods Enzymol.* **180,** 547−558.

6. Hutchins, C.J., Rathjen, P.D., Forster, A.C., and Symons, R.H. (1986) *Nucleic Acids Res.* 14, 3627–3640.
7. Epstein, L.M. and Gall, J.G. (1987) *Cell* 48, 535–543.
8. Haseloff and Gerlach (1989) *Gene* **82,** 43–52.
9. Uhlenbeck, O.C. (1987) *Nature* **328,** 596–600.
10. Haseloff, J. and Gerlach, W.L. (1988) *Nature* **334,** 585–591.
11. Koizumi, M., Iwai, S., and Ohtsuka, E. (1988) *FEBS Letters* **228,** 228–230.
12. Ruffner, D.E., Dahm, S.C. and Uhlenbeck, O.C. (1989) *Gene* **82,** 31–41.
13. Fedor, M.J. and Uhlenbeck, O.C. (1990) *Proc. Natl. Acad. Sci. USA* **87,** 1668–1672.
14. Ruffner, D.E., Stormo, G.D., and Uhlenbeck, O.C. (1990) *Biochemistry* **29,** 10695–10702.
15. Sheldon, C.C., and Symons, R.H. (1989) *Nucleic Acids Res.* **14,** 5679–5685.
16. Heus, H.A., Uhlenbeck, O.C., and Pardi, A. (1990) *Nucleic Acids Res.* **18,** 1103–1108.
17. Miller, W.A., Hercus, T., Waterhouse, P.M. and Gerlach, W.L. (1991) *Virology* **183**, 711–720.
18. Kunkel, T.A., Roberts, J.D. and Zakour, R.A. (1987) *Methods Enzymol.* **154,** 367–382.
19. Sambrook, J., Fritsch, E.F. and Maniatis, T. (1989) Molecular Cloning: A Laboratory Manual. Second edition. Cold Spring Harbor Laboratory Press, Cold Spring Harbor.
20. Conway, L. and Wickens, M. (1989) *Methods Enzymol.* **180,** 369–379.
21. Donis-Keller, H., Maxam, A.M. and Gilbert, W. (1977) *Nucleic Acids Res.* **8,** 3133–3142.
22. Simoncsits, A., Brownlee, G.G., Brown, R.S., Rubin, J.R. and Guilley, H. (1977) *Nature* **269,** 833–836.
23. Cedergren, R., Gautheret, D., Lapalme, G. and Major, F. (1988) *CABIOS* **4**, 143–146.
24. Vary, C.P.H., and Vournakis, J.N. (1984) *Nucleic Acids Res.* **12,** 6763–6778.
25. Lockard, R.E. and Kumar, A. (1981) *Nucleic Acids Res.* **9,** 5125–5140.
26. Lowman, H.B. and Draper, D.E. (1986) *J. Biol. Chem.* 261, 5396–5403.
27. Perotta, A.T and Been, M.D. (1991) *Nature* **350,** 434–436.
28. Rosenstein, S.P. and Been, M.D. (1990) *Biochemistry* **29,** 8011–8016.
29. Puglisi, J.D., Wyatt, J.R. and Tinoco Jr, I. (1988) *Nature* **331,** 283–286.
30. Knapp, G. (1989) *Methods Enzymol.* **180,** 192–213.
31. Pleij, C.W.A., Rietveld, K. and Bosch, L. (1985) *Nucleic Acids Res.* **13,** 1717–1731.
32. Epstein, L.M., and Pabon-Pena, L.M. (1991) *Nucleic Acids Res.* **19,** 1699–1705.
33. Davies, C., Sheldon, C.C., and Symons, R.H. (1991) *Nucleic Acids Res.* **19,** 1893–1898.
34. Forster, A.C., Davies, C., Sheldon, C.C., Jeffries, A.C., and Symons, R.H. (1988) *Nature* **334,** 265–267.
35. Sheldon, C.C., and Symons, R.H. (1989) *Nucleic Acids Res.* **14,** 5665–5677.
36. Tinoco Jr., I., Davis, P.W., Hardin, C.C., Puglisi, J.D., Walker, G.T., and Wyatt, J. (1987) *Cold Spring Harbor Symp. Quant. Biol.* **52,** 135–146.
37. Singleton, C.K., Klysik, J., Stirdivant, S.M., and Wells, R.D. (1982) *Nature* **299,** 312–316.
38. Zarling, D.A., Calhoun C.J., Hardin, C.C., and Zarling, A.H. (1987) *Proc. Natl. Acad. Sci. USA* 84, 6117–6121.
39. Zarling, D.A., Calhoun C.J., Feuerstein, B.G., and Sena, E.P. (1990) *J. Mol. Biol.* 211, 147–160.
40. Freier, S.M., Kierzek, R., Jaeger, J.A., Sugimoto, N., Caruthers, M.H., Neilson, T. and Turner, D.H. (1986) *Proc. Natl. Acad. Sci. USA* **83,** 9373–9377.
41. Schulz, V.P. and Reznikoff, W.S. (1990) *J. Mol. Biol.* 211, 427–445.